Pressure-Induced Phase Transformations in $LiAlH_4$

Raja S. Chellappa and Dhanesh Chandra*

Metallurgical and Materials Engineering Division (MS 388), University of Nevada, Reno, Nevada 89557

Stephen A. Gramsch and Russell J. Hemley

Geophysical Laboratory, Carnegie Institution of Washington, 5251 Broad Branch Road, NW, Washington, DC 20015

Jung-Fu Lin

Lawrence Livermore National Laboratory, 7000 East Avenue, Livermore, California 94550

Yang Song

Department of Chemistry, The University of Western Ontario, London, Ontario, Canada N6A 5B7

Received: January 23, 2006; In Final Form: April 5, 2006

The pressure-induced phase transformations in pure $LiAlH_4$ have been studied using in situ Raman spectroscopy up to 7 GPa. The analyses of Raman spectra reveal a phase transition at approximately 3 GPa from the ambient pressure monoclinic α-$LiAlH_4$ phase ($P2_1/c$) to a high pressure phase (β-$LiAlH_4$, reported recently to be monoclinic with space group $I4_1/b$) having a distorted $[AlH_4]^-$ tetrahedron. The Al−H stretching mode softens and shifts dramatically to lower frequencies beyond the phase transformation pressure. The high pressure β-$LiAlH_4$ phase was pressure quenchable and can be recovered at lower pressures (∼1.2 GPa). The Al−H stretching mode in the quenched state further shifts to lower frequencies, suggesting a weakening of the Al−H bond.

I. Introduction

The group of complex alkali aluminohydrides (so-called alanates) with the general formula $MAlH_4$ (M = Li, Na) are particularly attractive as potential candidates for hydrogen storage due to their high theoretical hydrogen weight content ($LiAlH_4$, for example, has 10.5 wt % hydrogen). Bogdanovic et al.[1,2] discovered that addition of suitable catalysts (Ti-based) to $NaAlH_4$ enhanced the hydriding kinetics and reduced the decomposition temperature, as well as promoted reversibility. This pioneering work led to the development of a class of hydrogen storage materials called catalyzed alanates, and recent research has focused on the selection and effective addition of catalysts to alanates. Similar to $NaAlH_4$, improvements in the hydriding properties of catalyzed $LiAlH_4$ and Li_3AlH_6 have been reported.[3−5] In general, the dehydrogenation reactions of $MAlH_4$ (M = Li, Na) are given below[6,7]

$$3MAlH_4 \rightarrow M_3AlH_6 + 2Al + 3H_2 \quad (1)$$

$$M_3AlH_6 \rightarrow 3MH + Al + \frac{3}{2}H_2 \quad (2)$$

Both LiH and NaH are not considered available for practical purposes due to the relatively high thermal stability of these compounds. For pure $LiAlH_4$, the decomposition temperatures for steps 1 and 2 are given to be 150−175 and 180−220 °C, with release of 5.3 and 2.6 wt % H_2, respectively. An overview of the development of catalyzed alanates can be found in Gross et al.,[8] and some outstanding issues about the reaction mechanisms of decomposition have been elucidated in Balema and Balema.[9]

Solid-state addition of catalysts (usually Ti-based) to alanates via high energy ball milling is now the preferred mode of synthesizing catalyzed alanates despite some loss of hydrogen content. The reduction in particle size and the availability of increased surface area for catalyst action are expected to aid in the hydriding kinetics of the complex hydrides. Although numerous reports can be found in the literature about addition of various catalysts to alkali aluminohydrides and the subsequent improvements in hydriding/dehydriding properties, the mechanochemical solid-state transformations in the hydride accompanying ball milling are still not well understood.[9] High energy ball milling is a dynamic mixing process where colliding ceramic or hardened steel balls in a confined volume crush and mix the catalyst and the hydride, resulting in solid-state transformations. The local stresses developed due to the collision of balls can result in the solid (getting crushed) experiencing pressures up to several gigapascals (reported to be as much as 6 GPa[10,11]). These stresses may indeed produce structural transformations[12] in the ball milled material or even result in the formation of new compounds if the ball milling is carried out in the presence of a catalyst.

The stability of pure and catalyzed $LiAlH_4$ after ball milling has been studied by many researchers.[13−16] However, these early studies focused on the mechanochemical activation and decomposition of $LiAlH_4$ during ball milling and did not report the effect on the dehydrogenation characteristics of $LiAlH_4$ due to

* Corresponding author. E-mail: dchandra@unr.edu. Phone: (775) 784-4960. Fax: (775) 784-4316.

10.1021/jp060473d CCC: $33.50
Published on Web 05/20/2006

TABLE 1: High Pressure (Room Temperature and High Temperature) Phase Transformation of $LiAlH_4$[a]

phase transformations	reference
α-$LiAlH_4$ monoclinic ($P2_1/c$) $a = 4.8174$, $b = 7.8020$ $c = 7.8214$, $\beta = 112.228°$ $\xrightarrow{2.6\ GPa}$ β-$LiAlH_4$ tetragonal ($I4_1/a$) $\xrightarrow{33.8\ GPa}$ γ-$LiAlH_4$ orthorhombic ($Pnma$)	Vajeeston et al.[18]
α-$LiAlH_4$ monoclinic ($P2_1/c$) $\xrightarrow[room\ temp]{2.2-3.5\ GPa}$ β-$LiAlH_4$	Talyzin and Sundquist[22]
α-$LiAlH_4$ monoclinic ($P2_1/c$) $\xrightarrow[room\ temp]{\sim 3\ GPa}$ β-$LiAlH_4$	this work
α-$LiAlH_4$ monoclinic ($P2_1/c$) $\xrightarrow[250-300\ °C]{7\ GPa}$ β-$LiAlH_4$ tetragonal $a = 6.75$, $c = 8.081$ $\xrightarrow[500\ °C]{7\ GPa}$ γ-$LiAlH_4$ orthorhombic ($Pnma$) $a = 5.11$, $b = 9.21$ $c = 4.29$	Bulychev et al.[19]
α-$LiAlH_4$ monoclinic ($P2_1/c$) $\rightarrow$ γ-$LiAlH_4$ monoclinic $a = 8.266$, $b = 5.530$ $c = 9.288$, $\beta = 90.72°$	Bastide et al.[20]

[a] Only the experimental lattice parameters are given from Hauback et al.[36] The calculated lattice parameters of the predicted room temperature high pressure phases can be found in Vajeeston et al.[18] The transformation pressures and temperatures from Bulychev et al.[19] and Bastide et al.[20] are from ex situ experiments. The experimental conditions at which Bastide et al.[20] observed their high pressure, high temperature phase transition was not clear. All lattice parameters are given in angstroms.

ball milling. In a recent systematically conducted study, Andreasen et al.[17] found that the dehydrogenation of ball milled $LiAlH_4$ exhibited significantly faster kinetics than unmilled $LiAlH_4$. In addition to the reduction in particle size, it is expected that some pressure-induced changes in Al−H bonding could also have a role in the faster dehydrogenation kinetics of the milled $LiAlH_4$. Therefore, a detailed study on the effect of pressure on the bonding and structure of $LiAlH_4$ is highly desirable. The interest in high pressure phase transformations of $LiAlH_4$ has also been renewed by a theoretical prediction of a high pressure phase at room temperature by Vajeeston et al.[18] At approximately 2.6 GPa, they predicted a transformation from an ambient pressure α-$LiAlH_4$ ($P2_1/c$, $Z = 4$) phase to a high pressure β-$LiAlH_4$ ($I4_1/a$, $Z = 4$) phase with a large volume collapse (>17%). If such a large volume collapse can be determined experimentally (from lattice parameters) and if the high pressure phase can be retained at ambient pressure by a rapid reduction in pressure (pressure quenching) or other chemical means, then this would lead to a new dense hydrogen storage material with gravimetric as well as volumetric efficiency.

The earliest high pressure studies on $LiAlH_4$ by Bulychev et al.[19] and Bastide et al.[20] were ex situ experiments using a belt-type apparatus that involved the application of both high pressure and temperature. The results from these studies are summarized in Table 1 along with the crystal structure parameters of the all the known high pressure (room temperature and high temperature) phases of $LiAlH_4$. The important conclusion from these previous studies was the change in coordination number of Al^{3+} from 4 to 6 in the high pressure phase due to the formation of $[AlH_6]^{3-}$ octahedra. Bureau et al.[21] also stated that the high pressure, high temperature phase possessed irregular $[AlH_6]^{3-}$ octahedra similar to the regular octahedral arrangement in Li_3AlH_6. Balema et al.[16] also suggested that ball milling of $LiAlH_4$ in the presence of Ti-based catalysts could lead to a rearrangement of the tetrahedral $[AlH_4]^-$ ion to octahedral $[AlH_6]^{3-}$ and alluded to the similarity with the high pressure, high temperature metastable γ-$LiAlH_4$ phase reported by the early researchers.[19,20]

Recently, the prediction of Vajeeston et al.[18] was tested by Talyzin and Sundquist[22] by performing high pressure in situ Raman spectroscopy in which they found a slow reversible phase transition between 2.2 and 3.5 GPa. To avoid nomenclature confusion, in this study, in accordance with Vajeeston et al.[18] and Talyzin and Sundquist,[22] the high pressure, room temperature phase is designated as β-$LiAlH_4$ in a departure from Bulychev et al.[19] and Bastide et al.[20] In their high pressure diamond anvil cell (DAC) experiments, Talyzin and Sundquist[22] used 4:1 methanol/ethanol as their pressure transmitting medium; however, it has been previously shown by Haubenstock and Mester[23] that there is some reactivity of $LiAlH_4$ with alcohols that involve partial substitution of H by an −OR functional group, where R is the alkyl group. The following reactions of alcohols with $LiAlH_4$ have been suggested:[23]

$$LiAlH_4 + x\mathrm{ROH} \rightleftharpoons LiAlH_{4-x}(\mathrm{OR})_x + xH_2 \qquad (3)$$

In the presence of a small amount of alcohol, the alkoxide derivative on the product side can partially dissociate with the presence of one, two, or three Al−H bonds. Thus, an intense Al−H stretching (even bending) mode can still be observed. However, the presence of other Raman signatures due to $-O-CH_3$ can still be weak or superimposed with some modes from the sample spectra. The effect of alcohol pressure media on the Raman spectra may not be dramatic in the high frequency region due to the above reasoning. However, the effect of the above reaction may be more on the low frequency librational and translational modes, affecting their intensity as well as frequency due to the partial substitutions in the molecular unit. The translational and librational modes are also of interest to understand the effect of pressure on the rigid $[AlH_4]^-$ unit. Also, Talyzin and Sundquist[22] have pointed out that they were unable to follow the low frequency lattice translational and librational modes as a function of pressure. As the first part of a systematic study on the high pressure behavior of $LiAlH_4$, we have conducted high pressure in situ Raman spectroscopy using a DAC on pure $LiAlH_4$ with the following objectives:

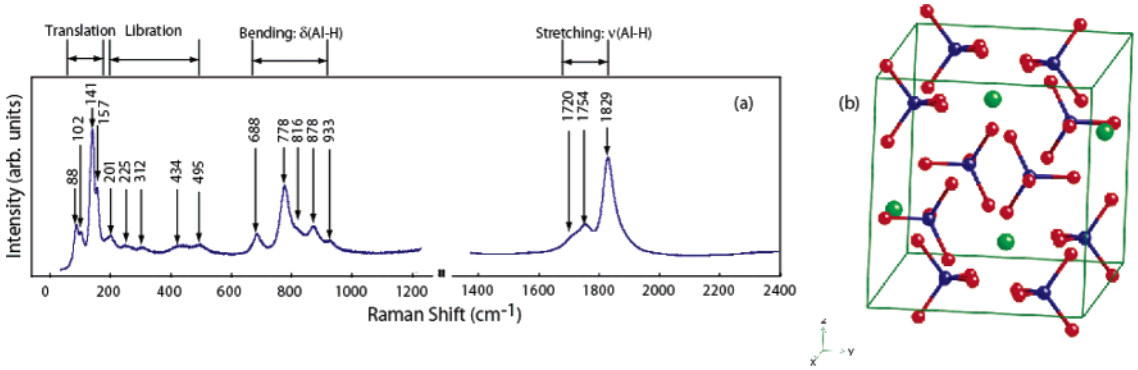

Figure 1. (a) Mode assignments for $LiAlH_4$ from this study (as-loaded sample (~0 GPa) in the DAC) showing the various vibrational modes. It is notable that the low frequency translational and librational (hindered rotation) modes are also well resolved. A nonlinear-regression-based multipeak fitting routine[30] was used to identify shouldered peaks. (b) The crystal structure of α-$LiAlD_4$ (red, D; blue, Al; green, Li) obtained from our neutron diffraction experiments.[38]

(1) To determine the phase transition pressure of $LiAlH_4$ at room temperature by loading multiple samples in a DAC without any pressure transmitting medium.

(2) To monitor the evolution of lattice (translational, librational), Al−H bending, and Al−H stretching modes as a function of pressure.

(3) To determine if the high pressure phase can be quenched to a lower pressure and ascertain its stability.

II. Experimental Procedure

Reagent grade $LiAlH_4$ powder of 95% purity was purchased from Sigma Aldrich Inc. and was used without further purification. The high pressure Raman spectroscopy experiments performed in this work were carried out at the Geophysical Laboratory (GL) at the Carnegie Institution of Washington (CIW), Washington, DC. The DAC used for the Raman spectroscopy[24] studies had diamonds with 500 μm culets, and samples were loaded in a rhenium gasket hole of about 140 μm. The powder form of $LiAlH_4$ was preferred, since the sample loading was performed in a glovebox (argon atmosphere) without any pressure transmitting medium. As mentioned earlier, a commonly used pressure transmitting medium such as 4:1 methanol/ethanol could have interactions with $LiAlH_4$, and it is also not possible to use them inside a glovebox. The ruby (Cr^{3+} doped α-Al_2O_3) fluorescence method (R_1 line at 694.2 nm under ambient conditions and shifting to higher frequencies with pressure) was used to determine the pressure inside the DAC.[25] A few ruby chips were spread along with the sample for monitoring the pressure. Since no pressure medium was used, the non-hydrostaticity is of concern. This was a reason to collect Raman spectra from multiple sample loadings to make sure that the transformation pressure was not over corrected. The sharp presence of both R_1 and R_2 ruby lines (for the relatively low pressures of this study) is a reasonable indication of the absence of large pressure gradients. Detailed analysis regarding the relative shift of the R_1 and R_2 lines can provide further information about the pressure gradient but was not performed in this study. The DAC was assembled and sealed with minimal initial pressure. Raman measurements were performed using the 514.5 nm green lines of an argon ion laser (Coherent Innova 90). A resolution of 0.5 cm^{-1} was achieved using a 460 mm focal length f/5.3 imaging spectrograph (ISA HR460) with an 1800 grooves/mm grating and liquid nitrogen cooled CCD detector (Princeton Instruments). The Raman scattering wavelength was calibrated using Ne lines, and a small offset correction was made to the observed Ne lines.[26] We note here that the Raman active modes near the first-order diamond peak at 1331 cm^{-1} cannot be studied due to the very high intensity of this peak. Therefore, spectra were collected for the ranges 100−1200 and 1400−3600 cm^{-1}.

After each pressure increment, the sample was allowed to stabilize for $^1/_2$−1 h and then the Raman spectrum was obtained. To obtain a well-resolved, smooth Raman spectrum, the collection time for the spectrum was 60 s. Care was ensured to attenuate the laser power to avoid any laser effect on the sample. Once a maximum pressure of about 5 GPa (for one run, the maximum pressure reached was 6.8 GPa) was reached, the pressure was decreased rapidly to about ~1.2 GPa. The sample was allowed to sit for at least 3 h before obtaining the spectra of the pressure quenched sample. Three sample runs were performed, and for one sample run, the quenched sample was held at a constant load for about 6 days inside the glovebox.

III. Results and Discussion

III.A. Vibrational Mode Assignment of Pure $LiAlH_4$. The complete description of the various vibrational modes can be useful for an in situ vibrational spectroscopy study of the decomposition of $LiAlH_4$. The first complete vibrational assignment for $LiAlH_4$ was reported by Bureau et al.[29] in 1985. The spectrum reported in this study provides the second known complete vibrational assignment for $LiAlH_4$ (from 80 to 2200 cm^{-1}). The vibrational mode assignment of the as-loaded $LiAlH_4$ sample in the DAC from this study is shown in Figure 1a, and the crystal structure of $LiAlD_4$ is shown in Figure 1b. The lattice parameters and atom positions used for computer simulation of the crystal structure shown in Figure 1b were obtained from our neutron diffraction studies.[38] We were able to obtain high resolution spectra and clearly identify bands of peaks corresponding to the lattice, bending, and stretching modes. The raw data obtained were first smoothed using a fast Fourier transform (FFT) smoothing routine.[30] The peaks were then directly extracted from the smoothed curve. It was found that a 15-point FFT smoothing was sufficient for Al−H bending and stretching mode regions, while a 10-point FFT smoothing (sometimes 5-point) was necessary to extract peaks for the lower wavenumber regions of translational and librational modes.

The Al−H bond dictates the vibrational mode characteristics of alkali metal aluminohydrides ($LiAlH_4$, $NaAlH_4$, and $KAlH_4$) and is evident from the fact that the Raman spectrum of $LiAlH_4$ is very similar to that of $NaAlH_4$.[27,28] The Raman spectrum of $LiAlH_4$ can be divided into four spectral regions in order of increasing frequency corresponding to translational, librational, bending (δ), and stretching (ν) modes. For comparison purposes, a compilation of the vibrational mode assignments from this

TABLE 2: Compilation of the Vibrational Mode[a] Assignment of $LiAlH_4$ from Experimental Raman Data

DAC as-loaded (this work)	peak intensity	DAC as-loaded (2004)[b]	powder Raman[29] (1985)	Raman in ether soln[35] (1973)	Raman in ether soln[34] (1956)	neutron scattering[31−33]	powder Raman of $NaAlH_4$[27] (2005)	vibrational mode assignments
88	m		95				107	
102	w-sh		112				116	
141	s		143			140	174	translational
157	w-sh		151			210, 240		
201	m		165			355		
225	w		220				419	
312	w		322				511	librational
434	w to m		438			467, 472		
495	w to m		510					
688	m	689	690	675			765	$\delta(AlH_2)$
778	s	779	780	783	782		847	sym-$\delta(AlH_2)$
816	w-sh	824	830				812	$\delta(AlH_2)$
878	w to m	873	882	880				$\delta(AlH_2)$
933	w	923	950					$\delta(AlH_2)$
1720	w-sh	1709	1722	1724				ν(Al−H)
1754	m	1753	1762	1759			1680	antisym-ν(Al−H)
1829	s	1832	1837	1838	1832		1769	sym-ν(Al−H)

[a] Units in inverted centimeters. [b] Talyzin and Sundquist[22] did not report any vibrational mode assignments below 500 cm^{-1}.

study along with those reported in the literature is given in Table 2. Since the alkali metal would not have a strong role in the vibrational mode behavior of the Al−H bond, the mode assignment of $NaAlH_4$ from Ross et al.[28] is also given in Table 2. The discussion of the vibrational mode assignment of $LiAlH_4$ is presented below for the four spectral regions.

III.A.1. Translational Modes. The low frequency region corresponding to wavenumbers from 80 to 160 cm^{-1} is assigned to the relative translational motion of the Li^+ and $[AlH_4]^-$ tetrahedra. There are two distinct peaks at 88 and 141 cm^{-1} with shoulders at 102 and 157 cm^{-1}, respectively. The peak at 201 cm^{-1} is also assigned to the translational mode. There is good agreement with the assignment of translational modes by Bureau et al.[29] It is also pointed out that, at ambient pressure and room temperature, the most intense vibrational mode is that of translation in both $LiAlH_4$ (141 cm^{-1}) and $NaAlH_4$ (174 cm^{-1}).

III.A.2. Librational Modes. The librational modes (hindered rotation) for $LiAlH_4$ are in the frequency region between 220 and 600 cm^{-1}. From the spectra obtained in this study, there are four librational modes at 225, 312, 434, and 495 cm^{-1}, which are in good agreement with those obtained by Bureau et al.[29] The librational motion in $LiAlH_4$ has been studied by incoherent neutron scattering by Temme and Waddington[31] who reported a strong peak at 470 cm^{-1} for $LiAlH_4$. This strong mode was attributed to the large vibrational amplitude of H in the $[AlH_4]^-$ tetrahedron, suggesting that the $[AlH_4]^-$ exists as a very stable ion that is rigidly locked in the crystal lattice. In another study, Gorbunov et al.[32] determined a librational mode at 472 cm^{-1} from the low temperature heat capacity measurements of $LiAlH_4$. It is also interesting to note that the frequencies for the torsional oscillations are rather high compared with the magnitude of other alkali aluminohydrides such as $KAlH_4$, $RbAlH_4$, and $CsAlH_4$. In fact, the librational mode for the $[AlH_4]^-$ ion in $KAlH_4$ determined by Tomkinson and Waddington[33] by inelastic neutron scattering is only 286 cm^{-1}.

III.A.3. Bending Modes {*δ(Al−H)*}. There are four distinct peaks at 688, 778, 878, and 933 cm^{-1} in the spectral region from 600 to 950 cm^{-1} that are due to the bending of Al−H bonds. The peak at 778 cm^{-1} has a shoulder at 816 cm^{-1}. These assignments are in good agreement with Bureau et al.[29] and Talyzin and Sundquist[22] as well as some earlier reports of $LiAlH_4$ in ether solutions.[34,35]

III.A.4. Stretching Modes {*ν(Al−H)*}. The high frequency spectral region is dominated by the Al−H symmetric peak at 1829 cm^{-1} and a shouldered antisymmetric peak at 1754 cm^{-1} (shoulder at 1720 cm^{-1}). These assignments are also in good agreement with those reported in the literature for $LiAlH_4$.

III.B. Raman Spectra of Pure $LiAlH_4$ as a Function of Pressure. Majzoub et al.[28] have shown that the behavior of Al−H modes in $NaAlH_4$ as a function of temperature provides important clues regarding the stability of the $[AlH_4]^-$ tetrahedron. They determined that the Al−H stretching modes do not show evidence of softening and remain intact even in the melt. The behavior of the Raman spectra as a function of pressure assumes significance in this regard as the effect of pressure on the Al−H bonds may be different from that of the temperature effect. The Raman spectra of $LiAlH_4$ as a function of pressure are shown in Figure 2. The spectra have been divided into two parts: Figure 2a depicts the Raman shift due to increasing pressure of the translational modes (88 cm^{-1} [sh 102 cm^{-1}], 141 cm^{-1} [sh 157 cm^{-1}], and 201 cm^{-1}), librational modes (225, 312, 434, and 495 cm^{-1}), and bending modes (688 cm^{-1}, 778 cm^{-1} [sh 816 cm^{-1}], 878 cm^{-1}, 933 cm^{-1}), and Figure 2b shows the Raman shift of the Al−H stretching modes (1829 and 1754 cm^{-1} [sh 1720 cm^{-1}]). As mentioned in the Experimental Procedure section, three separate runs were conducted to test the reproducibility of the Raman spectra behavior as a function of pressure, and the spectra are shown in Figure 2. It can be seen from Figure 2b that there is very good reproducibility between the three runs especially in the higher wavenumber regions. The translational and librational modes of the spectra in the region from 0 to 1200 cm^{-1} for run 1 were not as well resolved as the other two runs and hence are not included. This was most likely due to overcautious initial sealing (the initial pressure for run 1 was 1.4 GPa) of the DAC before transport out of the glovebox.

Selected peaks from various vibrational modes were monitored as a function of pressure to obtain a quantitative fit to the variation of the Raman shift as a function of pressure. From the knowledge of the isothermal bulk modulus (theoretical values for α-$LiAlH_4$ and β-$LiAlH_4$ taken from Vajeeston et al.[18]), the isothermal mode-Grüneisen parameter was determined for these vibrational modes. The isothermal mode-Grüneisen

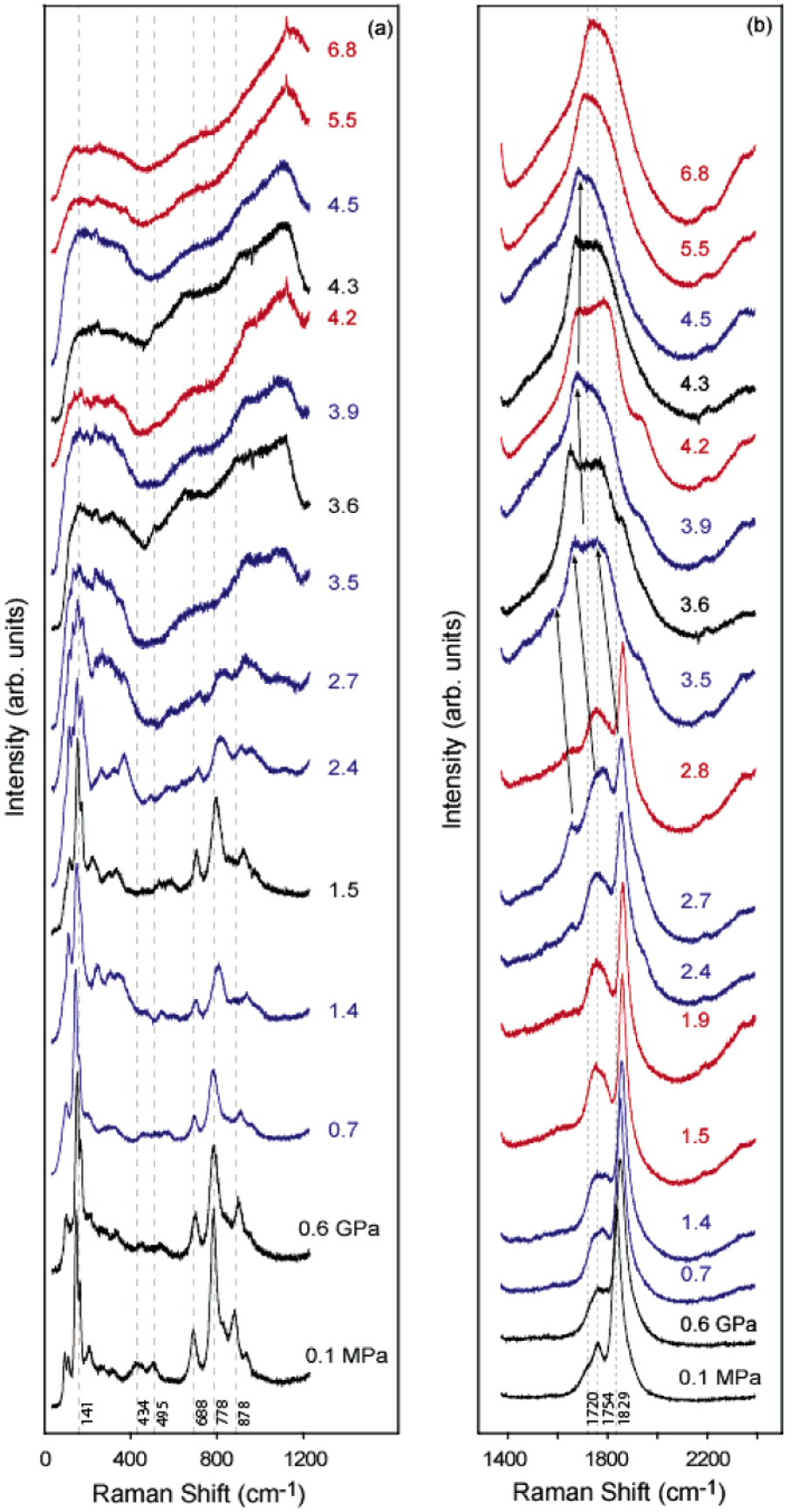

Figure 2. Raman spectra of pure $LiAlH_4$ as a function of pressure (a) from 0 to 1200 cm^{-1} showing the Raman shifts of translational, librational, and Al−H bending modes, (b) Al−H stretching modes from 1400 to 2400 cm^{-1}. There are three separate color coded runs that have been superimposed (runs 1, 2, and 3 are shown in red, blue, and black, respectively). The translational and librational modes of run 1 were not well resolved and are not shown in part a. Regions I, II, and III highlight the three broad peaks corresponding to the merged translational, librational, and bending modes, respectively. Also, arrows are marked on the Al−H stretching modes of run 2 to show the Raman shift of the Al−H stretching modes.

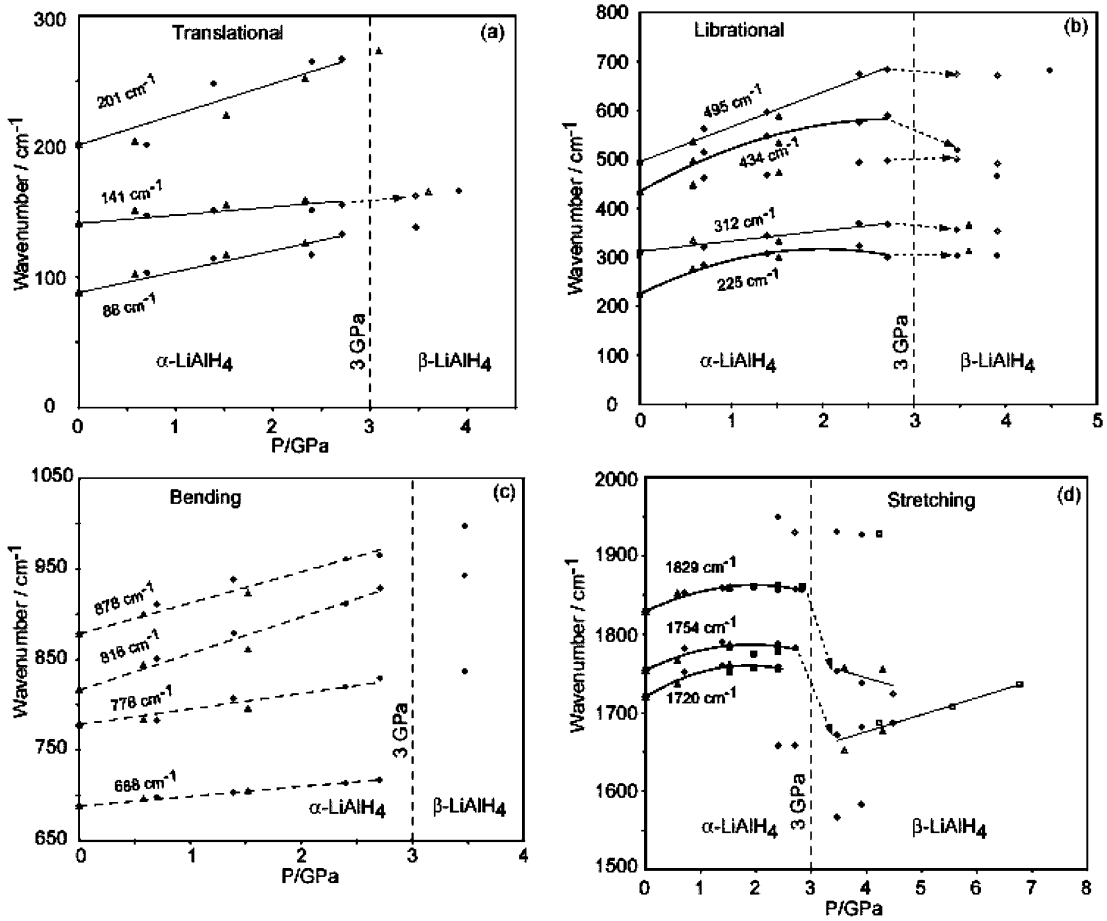

Figure 3. Raman shifts of (a) translational modes, (b), librational modes, (c) Al−H bending modes, and (d) Al−H stretching modes as a function of pressure. The large downward shift of the symmetric and antisymmetric Al−H stretching modes is shown by arrows. The shoulder for the antisymmetric Al−H stretching mode disappeared before the phase transition pressure. There are two peaks assigned to the β-$LiAlH_4$ phase that appear near the phase transition, one at about 1650 cm^{-1} and one at 1950 cm^{-1}, and disappear at higher pressures. The α-$LiAlH_4$ peaks are shown in solid symbols (runs 1, 2, and 3 are shown as squares, circles, and triangles, respectively), and the β-$LiAlH_4$ peaks are shown in open symbols. The Raman shifts of most modes were fit to be linear (σ (cm^{-1}) = $\sigma_0 + \sigma' P$); however, a parabolic fit (σ (cm^{-1}) = $\sigma_0 + \sigma' P + \sigma'' P^2$) is found to be useful[37] for some modes.

parameter for a vibrational frequency, ν_i, is given by the following relationship:[25]

$$\gamma_{iT} = -\frac{\mathrm{d} \ln \nu_i}{\mathrm{d} \ln V} = \frac{K_T}{\nu_i}\left(\frac{\partial \nu_i}{\partial P}\right)_T \qquad (4)$$

where K_T is the isothermal bulk modulus, V is the volume, and $(\partial \nu_i/\partial P)$ gives the rate of change of the vibrational frequency as a function of pressure. The above expression is typically evaluated from the Raman shift as a function of pressure. A discussion of the pressure-induced behavior of selected vibrational modes of $LiAlH_4$ is given in the following sections.

III.B.1. Translational and Librational Modes. The translational and librational modes of $LiAlH_4$ exhibit complex behavior as a function of pressure. The shoulder at 102 cm^{-1} merged into the stronger peak at 88 cm^{-1} upon initial compression to about 0.6 GPa. However, the most intense peak at 141 cm^{-1} and the shoulder at 157 cm^{-1} continue to be seen without significant loss of intensity to much higher pressures until the phase transformation pressure of ~3 GPa. This suggests that the crystal periodicity is still present due to an intact lattice, and these translational modes show an upward shift as the pressure is increased. The weak translational mode at 201 cm^{-1} initially shows a decrease in the intensity up to ~1 GPa but grows in intensity moving toward higher frequencies. The translational modes undergo a dramatic transformation between 2.7 and 3.6 GPa where all four translational modes appear to merge together with the two librational modes of lower frequencies. In fact, this transformation is clear at higher pressures (>4.5 GPa) where a broad, flattened peak extending from 50 to 300 cm^{-1} can be seen. The Raman shifts of translational modes at 88, 141, and 201 cm^{-1} were monitored as a function of pressure and plotted in Figure 3a. Other than the experimental scatter due to the two runs (runs 2 and 3), there is a linear trend in the α-$LiAlH_4$ translational modes with pressure. Beyond the phase transformation pressure of ~3 GPa, it was difficult to deconvolute the peaks due to the merging of translational modes into a broad peak. From the fit to the Raman shifts as a function of pressure, the isothermal mode-Grüneisen parameter for all of the vibrational modes was determined. As expected, the translational and librational modes have relatively higher mode-Grüneisen parameters than the Al−H bending and stretching modes. There is some uncertainty in the values determined here, as only the theoretical K_T value is available. It will be interesting to determine the intrinsic mode anharmonicities associated with the various vibrational modes from the knowledge of isobaric mode-Grüneisen parameters.

The librational modes at 225 and 312 cm^{-1} continue to shift to higher frequencies as the pressure is increased and merge on to the translational modes, forming a broad band. The behavior of the librational modes at 434 and 495 cm^{-1} is also interesting, as they shift to higher frequencies with a steeper $d\nu/dP$ gradient.

It does appear there is formation of new peaks (splitting of old peaks) around ~2.4 GPa in the frequency region between 350 and 700 cm^{-1}. However, due to their low intensities, they were not monitored as a function of pressure. At pressures around 2.4 GPa, the librational modes at 434 and 495 cm^{-1} begin merging with the lowest frequency bending mode at 688 cm^{-1}. This is significant, as the merged band appears to undergo a collective shift toward lower frequencies (mode softening) before a reduction in intensity at pressures greater than 5.5 GPa. Due to the merging of these modes, it was difficult to delineate peaks corresponding to the librations.

III.B.2. Bending and Stretching Modes. In addition to the intense translational mode at 141 cm^{-1}, the ambient pressure Raman spectra of pure α-$LiAlH_4$ are dominated by strong internal mode contributions from the δ(Al−H) bending and ν-(Al−H) stretching vibrations. The strong shouldered peak at 778 cm^{-1} continues to remain the most intense of all of the bending modes until ~2.4 GPa. At pressures between 1.5 and 2.4 GPa, the shoulder (816 cm^{-1}) from the 778 cm^{-1} peak emerges as a separate peak of equal relative intensity to the peak at 878 cm^{-1}. The weakest bending mode at 933 cm^{-1} displays a shift toward lower frequencies as it merges with the peak at 878 cm^{-1}. As mentioned in the discussion of the pressure behavior of the librational modes, the bending mode at 688 cm^{-1} merged with the two librational modes at 433 and 495 cm^{-1} and forms a collective broad band beyond 2.7 GPa. Beyond the phase transformation pressure of 3 GPa, the strongest bending mode peak at 778 cm^{-1} reduces dramatically in intensity. Briefly, the merged peak of 878 and 933 cm^{-1} is the strongest bending mode peak. It is apparent from the spectra at 3.5 GPa that the bending mode peaks at 778 cm^{-1} and the peaks due to merging of 878 and 933 cm^{-1} have shifted dramatically to higher frequencies with considerable broadening. In the high pressure β-$LiAlH_4$ phase, these modes do not exhibit any further mode softening. The Raman shift versus pressure for the bending modes is plotted in Figure 3c. The mode at 933 cm^{-1} was not monitored as a function of pressure, as the intensity of this mode was very low. However, it can be seen in Figure 2a that it does shift upward upon compression.

The Al−H stretching modes are the dominant vibrational characteristic, as expected in a compound with a stable $[AlH_4]^-$ tetrahedron. The shoulder adjoining the antisymmetric Al−H mode at 1720 cm^{-1} shifts toward higher frequencies, as shown in Figure 3d, and disappears (merges with the antisymmetric Al−H mode at 1754 cm^{-1}) beyond 2.4 GPa. There is a also a new peak that begins to develop at 1658 cm^{-1} around 2.4 GPa that is assigned to β-$LiAlH_4$, suggesting the beginning of a slow phase transformation to a high pressure phase. It is observed in this study that this new peak shows a large discontinuous downward shift beyond ~3 GPa. This behavior was not observed by Talyzin and Sundquist[22] who reported that this new peak persisted all the way up to their highest pressure of 6 GPa. In addition to this new peak, they also reported the continued presence of the two peaks corresponding to Al−H stretching modes up to their highest pressure of 6 GPa. It is pointed out that even in the current study the downward shift for the new peak was unequivocally observed only in one of the runs (run 2, marked by arrows in Figure 2). A parabolic fit was required for the regression of the Raman shift of the Al−H stretching modes as a function of pressure, as shown in Figure 3d.

The Raman shifts of the symmetric and antisymmetric stretching modes shows a parabolic increase up to the phase transformation and then a dramatic discontinuous downward shift to much lower frequencies. The mode at 1754 cm^{-1} increases to 1783 cm^{-1} at 2.7 GPa and lowers by more than 6% to 1672 cm^{-1} at 3.5 GPa, and beyond this pressure, it begins to increase with a slope of 21.57 cm^{-1}/GPa. The symmetric stretching mode at 1829 cm^{-1} shows a more complex behavior by downshifting from 1858 cm^{-1} at 2.8 GPa to 1753 cm^{-1} at 3.5 GPa and beyond this pressure continues to decrease to lower frequencies with a slope of −20.63 cm^{-1}/GPa. The mode-Grüneisen parameters are given in Table 3 for the stretching modes in the α-$LiAlH_4$ phase as well as in the high pressure β-$LiAlH_4$ phase. Due to the negative slope of the stretching mode in the high pressure phase, the mode-Grüneisen parameter is negative. It has to be pointed out that the Al−H stretching modes in the high pressure β-$LiAlH_4$ phase from 3.5 to 4.5 GPa appear to be a broad doublet peak and they could be weakly resolved corresponding to the antisymmetric and symmetric Al−H stretching modes. They do merge to form a single broad band beyond 5.5 GPa. Such complex behavior of the stretching modes was not observed by Talyzin and Sundquist[22] who showed the presence of three distinct broad peaks in the high pressure β-$LiAlH_4$ phase. It is not clear if the use of an alcohol-based pressure transmitting medium could explain the presence of the extra peaks in the high pressure β-$LiAlH_4$ phase in their[22] study.

TABLE 3: Raman Shifts as a Function of Pressure and Mode-Grüneisen Parameters for Selected Vibrational Modes of $LiAlH_4$[a]

α-$LiAlH_4$ ($P2_1/c$, K = 12.95 GPa)	
Raman modes at 1 atm (cm^{-1})	mode-Grüneisen parameter (γ)
88	2.4
141	0.6
201	1.5
225	5.3
312	0.9
434	3.2
495	1.9
688	0.2
778	0.3
816	0.6
878	0.5
1720	0.3
1754	0.2
1829	0.2
β-$LiAlH_4$ ($I2/b$,[39] K = 25.64 GPa)	
high pressure phase Raman modes extrapolated to 1 atm (cm^{-1})	mode-Grüneisen parameter (γ)
1590	0.3
1827	−0.3

[a] The mode-Grüneisen parameters were calculated using theoretical bulk moduli from Vajeeston et al.[18]

III.C. Pressure Quenching of the High Pressure β-$LiAlH_4$ Phase. The high pressure β-$LiAlH_4$ phase was pressure quenched after each of the three runs. The Raman spectra of the highest pressure of each run along with the "pressure quenched" sample are given in Figure 4. For comparison purposes, the ambient pressure (as-loaded) Raman spectrum is also shown. It can be seen in Figure 4a that the translational and librational modes have merged to form two broad peaks in the high pressure β-$LiAlH_4$ phase. After quenching and letting the sample stabilize in the DAC for about 3 h, the Raman spectra of the quenched sample (all three runs) show similar characteristics to those of the β-$LiAlH_4$ phase. It can be seen in Figure 2 that, in the high pressure β-$LiAlH_4$ phase, the librational and Al−H bending modes do not completely disappear but merge together to form a broad peak. The deconvolution of these modes was difficult,

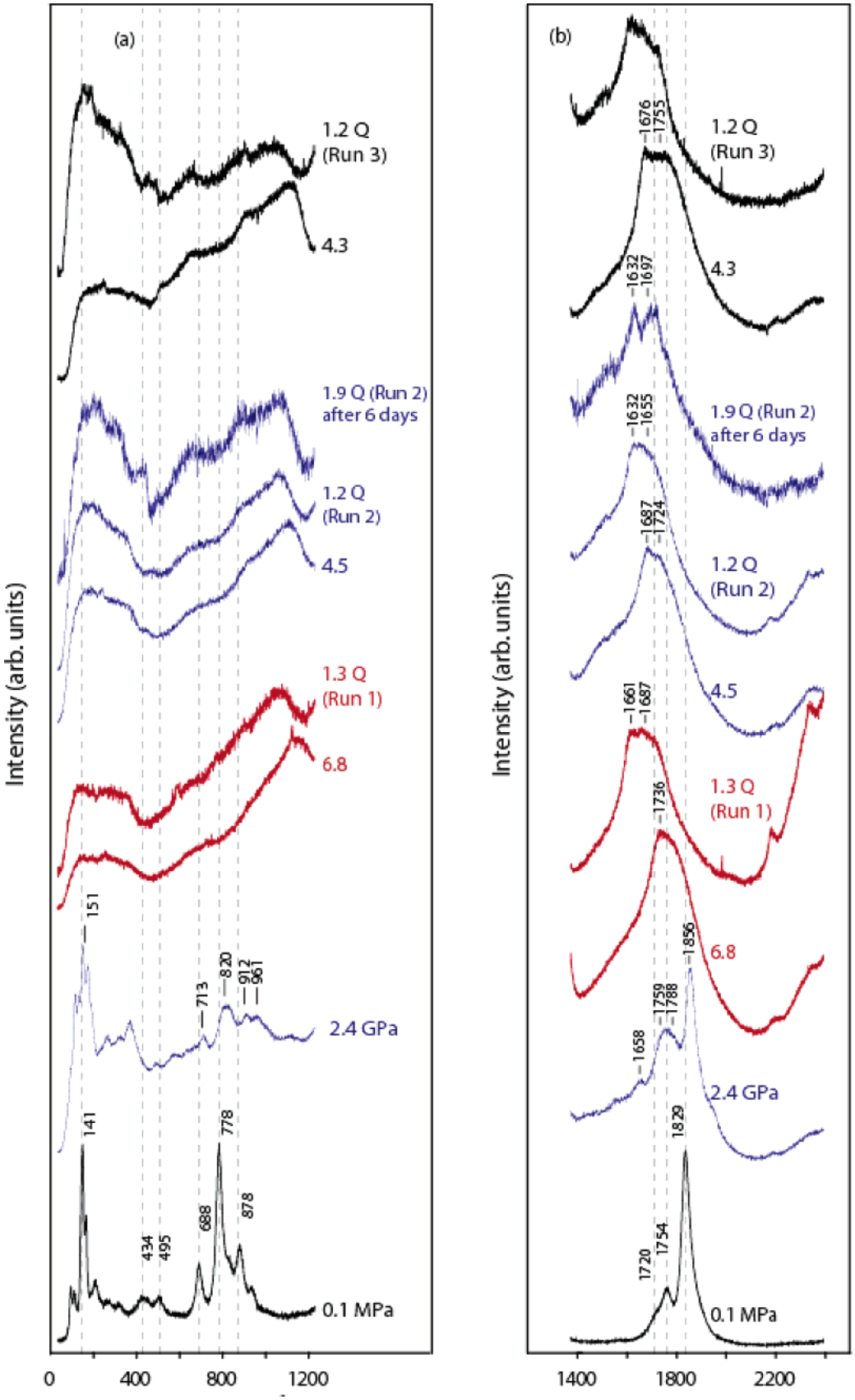

Figure 4. Raman spectra of the pressure quenched high pressure β-$LiAlH_4$ for the three separate pressure runs (runs 1, 2, and 3 are shown in red, blue, and black, respectively). Q denotes the quenched sample (spectra taken after 3 h).

but as shown in Figure 3b and c, some of these modes were monitored to as high of a pressure as possible. Upon pressure quenching, some of these modes were recovered in the quenched state. Obviously, it is not possible to completely release to ambient pressure, since it would damage the moisture sensitive sample. Therefore, the sample was quenched to a pressure (~1.2 GPa for runs 2 and 3 and ~1.3 GPa for run 1) that allowed the sample to remain sealed. For one of the runs (run 2), the sample

was allowed to remain in this quenched state for over 6 days. The pressure increased to 1.9 GPa after 6 days due to inherent mechanical relaxation of the DAC, and it can be seen in Figure 4a that some lattice modes are also beginning to appear.

The Al−H stretching modes show a much more dramatic behavior after pressure quenching. The behavior of these modes can provide important clues with regard to the strength of the Al−H bonds and therefore about the process of dehydrogenation. As mentioned earlier, the symmetric and antisymmetric Al−H stretching modes merged together to form a broad peak in the β-$LiAlH_4$ phase with a large downward shift in frequency at the phase transformation pressure, as shown in Figure 3d. Upon release of pressure, this broad peak undergoes a further shift toward lower frequencies. The symmetric stretching mode of the pressure quenched β-$LiAlH_4$ phase downshifts to shouldered peaks at 1655 cm^{-1} (1.2 GPa) for run 2 after 3 h and increases to 1697 cm^{-1} (1.9 GPa) after 6 days, to 1689 cm^{-1} (1.3 GPa) for run 1 after 3 h, and to 1687 cm^{-1} for run 3 (1.2 GPa) after 3 h. The antisymmetric stretching mode of the pressure quenched β-$LiAlH_4$ phase also downshifts to 1632 cm^{-1} (1.2 GPa) for run 2 after 3 h and remains at this wavenumber even after 6 days (1.9 GPa), to 1661 cm^{-1} (1.3 GPa) for run 1 after 3 h, and to 1617 cm^{-1} for run 3 (1.2 GPa) after 3 h. Rather interestingly, as can be seen from Figure 4, a low wavenumber peak between 1515 and 1540 cm^{-1} also appears in the pressure quenched β-$LiAlH_4$ phase. It is noted here that Talyzin and Sundquist[22] decompressed their sample in a stepwise fashion. They observed a complete reversibility of their phase transformation with a full recovery of the Al−H stretching modes at their ambient pressure frequencies. In this study, the pressure was released as rapidly as possible and the results are quite different in view of frequencies of the Al−H stretching modes after pressure release. High pressure synchrotron X-ray diffraction experiments will be able to verify whether β-$LiAlH_4$ is quenchable to ambient pressure.

III.D. Discussion. Recent research on catalyzed complex hydrides has been to explain the reaction mechanisms involved during catalysis and the subsequent improvement in hydrogen desorption/absorption kinetics. An understanding of the underlying phenomena will enable a theory-based process to improve the hydriding properties of the complex hydrides. Majzoub et al.[28] focused on understanding the vibrational mode behavior of $NaAlH_4$ as a function of temperature, to explain the necessary conditions for dehydrogenation of $NaAlH_4$. The two major findings by Majzoub et al.[28] are reiterated below:

(1) The lattice modes (translational and librational) of $NaAlH_4$ showed a shift toward lower frequencies (mode softening) as the temperature increased (disappearing in the melt due to loss of the $NaAlH_4$ lattice).

(2) The Al−H bending and stretching did not exhibit any noticeable mode softening, and $[AlH_4]^-$ was stable even in the melt, as evidenced by the strong Al−H stretching mode.

There are some interesting parallels/contrasts that can be drawn with the Raman study of $NaAlH_4$ as a function of temperature by Majzoub et al.[28] with the current study of $LiAlH_4$ due to the similar nature of the alkali aluminohydrides. The structural stability of the $[AlH_4]^-$ unit could inhibit the dehydrogenation, since release of hydrogen would have to involve the breaking of Al−H bonds. Majzoub et al.[28] have theorized that the role of the Ti catalyst could be to hasten the breaking of the Al−H bond to release hydrogen.

The effect of pressure on the lattice modes of $LiAlH_4$ is the opposite of the temperature effect, as the translational modes shift toward higher frequencies (until the phase transition) with a smaller $d\nu/dP$ gradient while the librational modes exhibit a slightly steeper $d\nu/dP$ gradient. However, in the high pressure β-$LiAlH_4$ phase, there is a noticeable merging of the translational and librational modes and there are two broad peaks corresponding to these merged modes, suggesting there may still be some long range order in the high pressure phase. After pressure quenching, some lattice modes appear again, as shown in Figure 4. However, the Al−H stretching modes show very interesting behavior as they undergo a pressure-induced phase transformation. First of all, just beyond the phase transition pressure of 3 GPa, the symmetric Al−H stretching mode at 1829 cm^{-1} shows a dramatic shift to lower frequencies and continues its downward trend in the high pressure phase. This may be an indication of the change in coordination number of the Al^{3+} ion from 4 to 6 associated with the formation of a distorted AlH_6 octahedron. There is also significant peak broadening of the Al−H stretching modes that is apparent looking at the high pressure β-$LiAlH_4$ spectra from 3.5 to 6.8 GPa and comparing them with the ambient pressure spectra. This considerable broadening of the peaks belonging to the internal modes (Al−H bending and stretching) as well as the emergence of one flat broad peak (which can be construed as a disappearance) corresponding to the lattice translational and librational modes suggests the possibility of at least partial amorphization in the high pressure β-$LiAlH_4$ phase. However, it is pointed out that some peak broadening can be attributed to the presence of pressure gradients due to non-hydrostaticity in the sample.

As mentioned earlier, the structure for the high pressure β-$LiAlH_4$ phase was theoretically predicted to be highly symmetrical tetragonal $I4_1/a$ (α-$NaAlH_4$ type). Talyzin and Sundquist[22] observed a triplet associated with Al−H stretching mode in the high pressure β-$LiAlH_4$ phase and concluded that the crystal structure could not be of the α-$NaAlH_4$ type, since the Raman spectra of the highly symmetrical α-$NaAlH_4$ have only two strong peaks. However, in this study, the Raman spectra of the high pressure β-$LiAlH_4$ phase in this study do not show evidence of a triplet in the Al−H stretching mode region. In fact, it can be seen from Figure 2, at pressures as high as 6.8 GPa, that there is only one broad peak in the Al−H stretching mode region.

Very recently, an article by Pitt et al.[39] reported the pressure-induced transformations in $LiAlD_4$ using neutron diffraction and determined the crystal structure of the high pressure β-$LiAlH_4$ phase to be monoclinic ($I2/b$) with lattice parameters of a = 4.099(3) Å, b = 4.321(4) Å, c = 10.006(7) Å, and γ = 88.43(2)° corresponding to a distorted $[AlH_4]^-$ tetrahedron. They also reported temperature effects up to 60 °C and determined that upon slow release of pressure and cooling there was a reversible phase transition back to α-$LiAlD_4$. Currently, we are planning high pressure synchrotron X-ray diffraction experiments on $LiAlH_4$ to redetermine the crystal structure of the high pressure β-$LiAlH_4$ phase as well to determine if the high pressure phase is retained after rapid release of pressure, as evidenced from our Raman studies.

It is also significant to note that, after the pressure quenching, there is a noticeable shift toward lower frequencies for the broad Al−H stretching mode peak. The negative mode-Grüneisen parameter for the symmetric stretching mode as a consequence of the mode softening in the high pressure β-$LiAlH_4$ phase is also interesting. This behavior of Al−H stretching modes both in the high pressure phase and especially after pressure quenching seems to indicate that there is some structural instability in $[AlH_4]^-$ that could enable the process of dehydrogenation. Also, as mentioned earlier, the mechanical milling

of alkali aluminohydrides does reduce the decomposition temperature; it will be informative to conduct dehydriding/hydriding experiments on the pressure quenched $LiAlH_4$. It is noted that since the phase transformation of $LiAlH_4$ is not very high in pressure (~3 GPa), synthesis of the high pressure phase (and subsequent quenching) in bulk, necessary for hydriding experiments, should not be difficult.

IV. Conclusions

Pressure-induced phase transformations at room temperature in pure $LiAlH_4$ have been investigated using in situ high pressure Raman spectroscopy. There is a phase transformation from ambient pressure monoclinic α-$LiAlH_4$ to β-$LiAlH_4$ at 3 GPa. The transformation pressure is close to the theoretically predicted value of 2.6 GPa as well as the previously reported transition pressures between 2.2 and 3.5 GPa. We were also successful in retaining the high pressure (β-$LiAlH_4$) phase by pressure quenching (rapid reduction in pressure) to a lower pressure of ~1.2 GPa. The Raman features of the quenched sample did not change appreciably with time. The stabilization of the high pressure phase at ambient pressure holds promise for developing novel hydrogen storage materials that are both volumetrically as well as gravimetrically efficient. However, the success of pressure quenching can be conclusively determined only after determining the crystal structure of the high pressure phase before and after quenching.

There is significant downshifting of the Al−H stretching modes to lower frequencies beyond the transition pressure. After rapid release of pressure, the Al−H stretching modes shift to even lower frequencies (no change after 6 days), suggesting further weakening of the Al−H bond. This behavior is very different from the behavior of the Al−H modes at higher temperatures where there was negligible softening of the Al−H stretching modes. The mode softening suggests a structural instability and a weaker Al−H bond at moderate pressures. Due to the high probability of similar structural changes (possibly an increased coordination number of Al^{3+} and the formation of AlH_6 octahedra) in ball milled $LiAlH_4$ or the static application of high pressure, it is hypothesized as a result of this study that the high pressure (quenched or otherwise) β-$LiAlH_4$ should possess enhanced dehydrogenation kinetics.

Acknowledgment. The authors would like to acknowledge the financial support of NSF (Grant No. 0132556) and Dr. Dennis Lindle of University of Nevada, Las Vegas, for his continuous support. J.-F.L. would like to thank U.S. DOE UC\LLNL (contract W-7405-Eng-48). R.S.C. and D.C. of University of Nevada, Reno, would like to thank the Carnegie/DOE Alliance Center (CDAC) for providing the opportunity to work as an academic collaborator.

References and Notes

(1) Bogdanovic, B.; Schwickardi, M. *J. Alloys Compd.* **1997**, *1*, 253−254.

(2) Bogdanovic, B.; Brand, R. A.; Marjanovic, A.; Schwickardi, M.; Tolle, J. *J. Alloys Compd.* **2000**, *302*, 36.

(3) Chen, J.; Kuriyama, N.; Xu, Q.; Takeshita, H. T.; Sakai, T. *J. Phys. Chem. B* **2001**, *105*, 11214.

(4) Slattery, D. K.; Hampton, M. D. *Hydrogen, Fuel Cells, and Infrastructure Technologies*; USDOE Progress Report FY 2003 "Complex hydrides for hydrogen storage".

(5) Chen, J.; Kuriyama, N.; Takeshita, H. T.; Sakai, T. *Adv. Eng. Mater.* **2001**, *3* (9), 695.

(6) Dilts, J. A.; Ashby, E. C. *Inorg. Chem.* **1972**, *11* (6), 1230.

(7) Dymova, T. N.; Aleksandrov, D. P.; Konoplev, V. N.; Silina, T. A.; Sizareva, A. S. *Russ. J. Coord. Chem.* **1994**, *20* (4), 279.

(8) Gross, K. J.; Majzoub, E. H.; Spangler, S. W. *J. Alloys Compd.* **2003**, *423*, 356−357.

(9) Balema, V. P.; Balema, L. *Phys. Chem. Chem. Phys.* **2005**, *7*, 1310.

(10) Maurice, D. R.; Courtney, T. H. *Metall. Mater. Trans. A* **1990**, *21*, 289.

(11) Weeber, A. W.; Wester, A. J. H.; Haag, W. J.; Bakker, H. *Physica B* **1987**, *145*, 349.

(12) Hemley, R. J.; Prewitt, C. T.; Kingma, K. J. *Rev. Mineral.* **1994**, *29*, 41.

(13) Balema, V. P.; Dennis, K. W.; Pecharksy, V. K. *Chem. Commun.* **2000**, *17*, 1665.

(14) Pecharsky, V. K.; Balema, V. P. In *Proceedings of Fundamentals of Advanced Materials for Energy Conversion*, TMS Annual Meeting and Exhibition, Seattle, WA, Feb 17−21, 2002; pp 95−107.

(15) Zaluski, L.; Zaluska, A.; Strom-Olsen, J. O. *J. Alloys Compd.* **1999**, *290*, 71.

(16) Balema, V. P.; Pecharsky, V. K.; Dennis, K. W. *J. Alloys Compd.* **2000**, *313*, 69.

(17) Andreasen, A.; Vegge, T.; Pedersen, A. S. *J. Solid State Chem.* **2005**, *178*, 3664.

(18) Vajeeston, P.; Ravindran, P.; Vidya, R.; Fjellvag, H.; Kjekshus, A. *Phys. Rev. B* **2003**, *68*, 212101.

(19) Bulychev, B. M.; Verbetskii, V. N.; Semenenko, K. N. *Russ. J. Inorg. Chem.* **1977**, *22* (11), 2961.

(20) Bastide, J.-P.; Bureau, J.-C.; Letoffe, J.-M. Claudy, P. *Mater. Res. Bull.* **1987**, *22*, 185.

(21) Bureau, J. C.; Bastide, J.-P.; Claudy, P.; Letoffe, J.-M.; Amri, Z. *J. Less-Common Met.* **1987**, *130*, 371.

(22) Talyzin, A. V.; Sundquist, B. *Phys. Rev. B* **2004**, *70*, 180101.

(23) Haubenstock, H.; Mester, T., Jr. *J. Org. Chem.* **1983**, *48*, 945.

(24) Raman, C. V.; Krishnan, K. S. *Nature* 1928, *121*, 711.

(25) Gillet, P.; Hemley, R. J.; McMillan, P. F. *Rev. Mineral.* **1998**, *37*, 525−581.

(26) Song, Y.; Hemley, R. J.; Mao, H. K.; Liu, Z.; Herschbach, D. R. *Chem. Phys. Lett.* **2003**, *382*, 686.

(27) Ross, D. J.; Halls, M. D.; Nazri, A. G.; Aroca, R. F. *Chem. Phys. Lett.* **2004**, *388*, 430.

(28) Majzoub, E. H.; McCarty, K. F.; Ozolins, V. *Phys. Rev. B* **2005**, *71*, 024118.

(29) Bureau, J.-C.; Bonnetot, B.; Claudy, P.; Eddaoudi, H. *Mater. Res. Bull.* **1985**, *20*, 1147.

(30) http://www.originlab.com.

(31) Temme, F. P.; Waddington, T. C. *J. Chem. Soc., Faraday Trans. 2* **1973**, *69*, 783.

(32) Gorbunov, V. E.; Gavrichev, K. S.; Sharpataya, G. A. *Russ. J. Inorg. Chem.* **1988**, *33*, 2678.

(33) Tomkinson, J.; Waddington, T. C. *J. Chem. Soc., Faraday Trans. 2* **1975**, *71*, 2065.

(34) D'Or, L.; Fuger, J. *Bull. Soc. R. Sci. Liege* **1956**, *25*, 14.

(35) Shirk, A. E.; Shriver, D. F. *J. Am. Chem. Soc.* **1973**, *95*, 5904.

(36) Hauback, B. C.; Brinks, H. W.; Fjellvåg, H. *J. Alloys Compd.* **2002**, *346*, 184.

(37) Perlin, P.; Jauberthie-Carillon, C.; Itie, J. P.; Miguel, A. S.; Grzegory, I.; Polian, A. *Phys. Rev. B* **1992**, *45*, 83.

(38) Chien, W.-M.; Chandra, D.; Huq, A.; Richardson, J. W., Jr.; Maxey, E.; Kunz, M.; Fakra, S. Neutron and Synchrotron Studies on Li-Based Nitride and Hydride, manuscript in preparation, 2005.

(39) Pitt, M. P.; Blanchard, D.; Hauback, B. C.; Fjellvåg, H.; Marshall, W. G. *Phys. Rev. B* **2005**, *72*, 214113.